

RSC Advances



This is an *Accepted Manuscript*, which has been through the Royal Society of Chemistry peer review process and has been accepted for publication.

Accepted Manuscripts are published online shortly after acceptance, before technical editing, formatting and proof reading. Using this free service, authors can make their results available to the community, in citable form, before we publish the edited article. This *Accepted Manuscript* will be replaced by the edited, formatted and paginated article as soon as this is available.

You can find more information about *Accepted Manuscripts* in the [Information for Authors](#).

Please note that technical editing may introduce minor changes to the text and/or graphics, which may alter content. The journal's standard [Terms & Conditions](#) and the [Ethical guidelines](#) still apply. In no event shall the Royal Society of Chemistry be held responsible for any errors or omissions in this *Accepted Manuscript* or any consequences arising from the use of any information it contains.

Table of contents entry



ZnO hollow microspheres exhibiting only *c* planes on the surface were successfully synthesized by a solvothermal method even without using template. The ZnO hollow microspheres are formed by preferential dissolution of centers of ZnO solid microspheres which have low crystallinity.

Template-Free Solvothermal Preparation of ZnO Hollow

Microspheres Covered with *c* Planes

Taiki Ihara¹⁾, Hajime Wagata²⁾, Toshihiro Kogure³⁾, Ken-ichi Katsumata¹⁾, Kiyoshi Okada¹⁾, and Nobuhiro Matsushita^{1)*}

¹⁾ Materials and Structures Laboratory, Tokyo Institute of Technology, 4259 Nagatsuta, Midori-ku, Yokohama 226-8503, Japan

²⁾ Department of Environmental Science and Technology, Shinshu University, 4-17-1 Wakasato, Nagano 380-8553, Japan

³⁾ Department of Earth & Planetary Science, Graduate School of Science, The University of Tokyo, 7-3-1 Hongo, Bunkyo-ku, Tokyo 113-0033, Japan

*Corresponding Author

Nobuhiro Matsushita
Materials and Structures Laboratory, Tokyo Institute of Technology, 4259 Nagatsuta, Midori-ku, Yokohama 226-8503, Japan

Tel: (+)81-45-924-5310 Fax: (+)81-45-924-5358

E-mail: matsushita.n.ab@m.titech.ac.jp

Abstract

ZnO hollow microspheres were prepared by a solvothermal method, without using a template. The morphology and structure of the microspheres were investigated by scanning and transmission electron microscopies. A series of controlled experiments was carried out to better understand the formation mechanism. The sample prepared at 150 °C for 1 h consisted of ZnO microspheres 1–2 μm in diameter. Microspheres were composed of crystallites of tens of nm in diameter. The surfaces of the microspheres prepared at 150 °C for 3 h were surrounded by hexagonal pyramid-like crystals, of a few hundred nm in diameter. The sample prepared by reaction at 150 °C for 6 h consisted of hollow spheres, even in the absence of a template. The microsphere surface consisted of ZnO *c* planes. ZnO hollow microspheres prepared at 150 °C for 12 h exhibited intense narrow ultraviolet emission.

Key words: ZnO, solvothermal, hollow sphere, template-free

Introduction

Zinc oxide (ZnO) is an n-type semiconductor, with a wide direct band gap (3.37 eV) and large exciton binding energy (60 meV). ZnO has potential in many applications, because of its distinct optical and electronic properties.¹⁻⁷ ZnO has a wurtzite structure, and exhibits spontaneous electrical polarization along its *c* axis. The positive polar face (0001) is termed the *c*(+)-plane, and negative polar face (000 $\bar{1}$) the *c*(-)-plane, which are terminated with Zn and O atomic planes, respectively. The chemical stability and catalytic activity of ZnO depend on its polarity.⁸⁻¹⁰ The photocatalytic activity of ZnO strongly depends on the specific crystal planes involved. The (0001) and (000 $\bar{1}$) faces exhibit higher photocatalytic activity than the perpendicularly-orientated nonpolar (10 $\bar{1}$ 0) and (11 $\bar{2}$ 0) faces. Thus, ZnO morphologies predominantly exposing *c* planes are likely to exhibit good photocatalytic behavior. Matsumoto *et al.* reported ZnO solid microspheres covered with *c*(+)-planes.¹¹

The preparation of ZnO hollow spheres has received much attention, because of their low density, high surface area and good surface permeability.^{12,13} ZnO hollow spheres have potential in gas sensing, drug delivery, microcapsule reactors and photoelectric devices.¹⁴⁻¹⁶ They also exhibit large light-harvesting efficiencies, so are also applicable in photocatalysts and dye sensitized solar cells. ZnO hollow spheres with surface-exposed *c* planes are likely to exhibit better performance than ZnO solid microspheres. However, preparing well-crystallized ZnO

hollow microspheres with controlled surface morphologies and crystal orientations remains a challenge.^{17,18}

Thermal evaporation¹⁹⁻²¹ and template hydrothermal processing^{22,23} are commonly used to prepare ZnO hollow microspheres. The thermal evaporation process generally involves the vaporization of Zn powder, solidification of liquid Zn droplets, oxidation of spherical Zn particle surfaces, and sublimation of Zn within particles. Its disadvantages include the requirement for high temperatures (typically >500 °C) and vacuum conditions. The hydrothermal synthesis of ZnO hollow spheres is usually achieved by either hard²² or soft templating.²³ Such templates complicate the synthesis process, and often require subsequent removal steps. The development of facile, low temperature and template-free methods for preparing ZnO hollow spheres is desirable. Zhu *et al.* reported the template-free preparation of ZnO hollow spheres, in aqueous solution at low temperature.²⁴ Li *et al.* reported the template-free solvothermal preparation of ZnO hollow spheres, which was assisted by polyoxometalate.²⁵ However, these reports did not clarify the crystal orientation in the prepared hollow spheres. There have been few reports of ZnO spherical hollow powders with surfaces covered with *c* planes.^{26,27} Hu *et al.* prepared ZnO hollow microspheres consisting of ZnO nanorods with surface-exposed *c* planes, using a water/glycerol solvent.²⁶ Qui *et al.* prepared hierarchical Zn_{1-x}Co_xO nanodiscs into hollow spheres with surface-exposed *c* planes, using a

water/ethylene glycol solvent. However, further investigation is required to reveal the formation mechanism.²⁷

In the current study, we report the template-free solvothermal preparation of ZnO hollow microspheres, using ethylene glycol (EG) and hexamethylenetetramine (HMT) as the solvent and pH buffer, respectively. The synthetic process is simple, and does not require specialized equipment or templates. Highly crystalline microspheres are obtained at a solvothermal temperature of 150 °C. The morphology of the ZnO particles can be tuned from solid to hollow spheres, by varying the reaction time. The ZnO hollow spheres are covered with *c* planes. A formation mechanism is proposed, based on the Zn²⁺ solubility and microsphere inner structure.

Experimental Section

Synthesis of ZnO Hollow Microspheres

Zinc acetate dihydrate [Zn(CH₃COO)₂·2H₂O] (>99%, Wako Pure Chemical Industries, Japan), HMT [C₆H₁₂N₄] (>99%, Wako Pure Chemical Industries) and EG [C₂H₄(OH)₂] (>99.5%, Wako Pure Chemical Industries) were of reagent grade, and used without further purification. For the solvothermal synthesis of ZnO hollow microspheres, a closed cylindrical 35 ml polytetrafluoroethylene-lined stainless steel autoclave was used. In a typical synthesis, 3 mmol of Zn(CH₃COO)₂·2H₂O and 12 mmol of HMT were dissolved in a 30 ml solution of EG (95

vol.%) and distilled water (5 vol.%). The resulting solution was transferred to the autoclave and heated at 150 °C for 1–12 h. The precipitate was collected, thoroughly washed with ethanol, and dried at 60 °C.

Characterization

Crystal phases were determined by X-Ray diffraction (XRD), using a RINT2000 diffractometer (Rigaku, Japan) with Cu-K α radiation. Morphologies were observed by field-emission scanning electron microscopy (SEM) (S4500, Hitachi, Japan). Microstructures were analyzed by transmission electron microscopy (TEM) (JEM-2010UHR, JEOL, Japan), with an operating voltage of 200 kV. Cross-sections of ZnO microspheres were prepared using a focused ion beam (FIB) instrument (FB-2100, Hitachi). Microspheres on substrates were first coated with amorphous carbon, to prevent charging during FIB treatment and to allow clear TEM observations of the surface structure. Thick tungsten layer, around 1 μ m, was deposited by deposition gun for the protection. Cross-sections were thinned to \sim 100 nm, using a 10 keV Ga ion beam. The Zn²⁺ concentration of the supernatant after reaction was measured by inductively coupled plasma-atomic emission spectroscopy (ICP-AES) (ICPS-8100, SHIMADZU, Japan). Photoluminescence (PL) measurements were recorded at room temperature using a luminescence spectrometer (LS55, PerkinElmer Inc., USA), at an excitation of 325 nm.

Results and discussion

The morphologies of products prepared by solvothermal treatment at 150 °C for different reaction times were observed by SEM, as shown in Figure 1. Figure 1a shows an SEM image of ZnO obtained after reaction for 1 h, in which uniform solid microspheres 1–2 μm in diameter were observed. The high-magnification image in Figure 1b indicated that the ZnO spheres consisted of nanoparticles, of ~20 nm in diameter. Uniform microspheres were also obtained after reaction for 3 h (Figure 1c). In this case, particles on the spherical surfaces consisted of crystalline hexagonal platelets of ~200 nm in diameter (Figure 1d). Isolated hollow spheres were observed in the sample prepared for 6 h, as shown by the red arrows in Figure 1e. Figure 1f indicates that the shell thickness was 200–300 nm for the particles reacted for 6 hours, with a rougher surface appearance than the sample reacted for 3 h (Figures 1c and 1d). The number of hollow spheres increased with increasing reaction time, as shown in Figure 1g. XRD was used to determine the crystal structure of the products. Figure S1 shows the XRD patterns of samples obtained after different reaction times, at a constant reaction temperature of 150 °C. The observed diffraction peaks were in good agreement with those of hexagonal wurtzite ZnO (JCPDS No. 36-1451), even for the sample prepared after 1 h. No other peaks were detected, indicating the high purity of the samples.

Figure 2 shows the particle size distributions of spheres prepared at 150 °C for different

reaction times. Data were obtained from 500 individual spheres observed in SEM images. The mean particle size (standard deviation) for samples prepared for 1, 3 and 12 h were 2.3 (0.5), 3.1 (0.6) and 2.8 (0.6) μm , respectively. The particle size increased with reaction time from 1 to 3 h, because of crystal growth. The particle size of the sample prepared for 12 h was slightly lower, because of dissolution of the nanoparticles.

The size, shape and surface morphology of the solid and hollow microspheres were characterized by TEM. The TEM images of the products prepared for 3, 6 and 12 h dispersed on carbon films are shown in Figure 3. Contrast between the sphere edges and cores was not observed for the sample reacted for 3 h, indicating that the microspheres were solid (Figure 3a). Contrast between edges and the core was apparent in some spheres reacted for 6 h (Figure 3b). When the reaction time was 12 h, the shells appeared porous, and contrast between shells and cores was apparent for all spheres, indicating hollow structures (Figure 3c). Figure 4 shows SEM and corresponding cross-sectional TEM images of solid and hollow spheres prepared at 150 °C for 3 h (Figures 4a–c) and 12 h (Figures 4d and e). Solid spheres appeared dense, and a radial contrast was observed inside the sphere (Figure 4b). The region around the center of the sphere appeared porous, while that within ~500 nm of the surface appeared dense. Different crystal sizes were observed at the surface and core. A selected-area electron diffraction (SAED) pattern of an individual sphere exhibited a ring-like pattern, as shown inset in Figure 3b. This

indicated that the center was composed of polycrystalline ZnO, rather than being amorphous. A high-resolution TEM (HRTEM) image of a sphere surface (Figure 4c) showed clear and continuous lattice fringes, with spacing of 0.52 nm. This corresponds to the 0001 plane, and indicates that the surfaces of the spheres were covered with *c* planes. Figure 4e shows that the sample prepared for 12 h consisted of hollow microspheres, whose shells were composed of needle-like ZnO crystals.

The Zn concentration in the supernatants of reacted solutions was measured, to investigate the formation mechanism of the ZnO hollow microspheres. Figure 5 shows the variation of supernatant Zn concentration, measured by ICP-AES after each reaction duration at 150 °C. The Zn concentration at 3 h was lower than that at the beginning of the reaction, because Zn²⁺ was consumed during the formation of ZnO spheres. The concentration increased after 3 h, and became saturated by 9 h. This increase can be attributed to the dissolution of particles at the center of individual spheres.

The effect of reaction temperature on the formation of ZnO hollow microspheres was also investigated. For the sample prepared at 100 °C for 12 h, solid microspheres were clearly obtained, as shown in Figure 6. Their surfaces consisted of hexagonal crystals of hundreds of nm in diameter, and were similar to the surfaces of the sample prepared at 150 °C for 3 h (Figure 1d). An SEM image of a broken sphere revealed a solid hierarchical structure consisting

of pyramid-like crystals (Figure 6b). Microspheres prepared at 200 °C were composed of larger particles (Figure 6c), and an SEM image of one of these broken sphere revealed a hollow structure (Figure 6d). The shell was much thicker than that of the sample prepared at 150 °C. ICP-AES was also used to measure the variation of supernatant Zn concentrations for reactions at 100 and 200 °C (Figure S2). No precipitate was obtained after reaction for 1 h at 100 °C, and the Zn concentration was comparable to the initial Zn concentration (~6000 ppm). For reaction at 100 °C, the supernatant Zn concentration gradually decreased with increasing reaction time, because of the formation of ZnO. An increase in Zn concentration was not observed until a reaction time of 12 h. The supernatant Zn concentration exhibited an unstable change upon reaction at 200 °C. For reaction after 1 h, the Zn concentration was much lower than the initial concentration (~6000 ppm), and the concentration fluctuated with increasing reaction time. These results indicated that 150 °C was the optimal temperature for preparing ZnO hollow microspheres. This was because dissolution did not occur at lower reaction temperatures (100 °C), and the reaction was too fast to readily control at higher temperatures (200 °C). Figure 7 shows SEM images and corresponding cross-sectional TEM images of ZnO microspheres prepared at 200 °C for 1 and 4 h. A cross-sectional TEM image of the microspheres prepared at 200 °C reveals a clear difference between the sphere surfaces and centers. The cross-sectional TEM image of the sample prepared for 1 h in Figure 7b is similar to that of the sample prepared

at 150 °C for 3 h (Figure 3b). The center of the sphere appears porous, and the surface appears to be dense to a depth of ~200 nm. A high magnification TEM image of the sphere surface shown inset in Figure 7b indicates the surface consists of pyramid-like crystals. The HR-TEM image in Figure 7c shows that surface particles were single crystals with 0.52-nm-lattice fringes which correspond to the [0001] ZnO growth direction. This indicated that the surface of the ZnO spheres was covered with *c* planes. Figure 7d shows that the centers of spheres prepared by reaction for 4 h had started to become hollow. A difference in the sphere's structure was clearly observed from the center to surface, as the structure changed from granular, needle-like to pyramid-like crystals (Figure 7e). The surface of this sphere was surrounded by pyramid-like crystals 300–600 nm in diameter. Some surface crystals had side facets appearing as brilliant-cut diamonds, which are shown inset in Figure 7e. The well-resolved lattice fringes also indicate that the surface was highly crystalline with flat planes, as shown in Figure 7f.

Figure 8a shows a proposed mechanism for formation of the ZnO hollow microspheres, based on the SEM, TEM, XRD and ICP-AES results. The following reactions are proposed to have occurred in the first step of the formation of solid ZnO microspheres:





The role of HMT ($\text{C}_6\text{H}_{12}\text{N}_4$) in the growth of the solid microspheres can be regarded as a pH buffer, because it slowly releases OH^- during thermal decomposition (Eqs. 1 and 2).²⁸ OH^- reacts with Zn^{2+} to form Zn(OH)_2 nanoclusters in solution (Eq. 3), which subsequently transform into an initial ZnO crystal (Eq. 4). The initial crystals agglomerate after nucleation, to form ZnO solid microspheres and thus minimize their surface energy. Extended reaction time results in particles on or near the surface growing into hexagonal crystals. After the degree of supersaturation decreased, the following reaction occurred:



Particles at sphere centers possessing low crystallinity preferentially dissolved according to Eq. 5, and hollow spheres are formed through Ostwald ripening²⁹.

We investigated the optical properties of the ZnO hollow microspheres by room-temperature PL measurements. Figure 9 shows the PL spectrum of the ZnO hollow microspheres, which exhibited strong UV emission at ~ 392 nm. While weak emission was observed at ~ 420 nm, emission at visible wavelengths was negligible.^{26,30,31} The UV emission originated from the recombination of free excitons in the ZnO near band edge,³² so that the intensity of the room-temperature UV emission indicated the ZnO quality. Visible emission is associated with interstitial Zn ions,³³ oxygen vacancies,³⁴ cationic impurities³⁵ and damaged crystals.³⁶ Visible

emission indicates the existence of deep centers within the ZnO. Therefore, the strong band-edge emission accompanied by insignificant visible emission suggests that the ZnO hollow spheres were of high crystal quality. The effect of non-radiative recombination centers was not considered in the current study, so it should not be concluded that the ZnO hollow spheres had a lower defect concentration than previous studies.^{26,30,31} Further investigation of the total defect concentration of the ZnO hollow spheres is required.

Conclusion

A template-free solvothermal preparation of ZnO hollow microspheres is reported. The mean diameter of the ZnO hollow microspheres was 2.8 μm . A formation mechanism of the ZnO hollow microspheres is proposed, based on the morphological evolution observed by SEM, TEM and ICP-AES analyses during particle growth. Solid microspheres initially consisting of 10 nm particles were formed by the agglomeration of primary particles after nucleation. Surface particles on the solid microspheres then grew into hexagonal crystals. When the degree of saturation decreased, the low crystallinity sphere centers preferentially dissolved, and hollow microspheres were formed through Ostwald ripening. The microspheres were covered with ZnO *c* planes. These ZnO hollow microspheres may have applications in photocatalysis, dye sensitized solar cells, photonic crystals and advanced optoelectronic devices. The preparation described within may provide a new strategy for designing generic hollow materials.

Acknowledgments

We thank Ms. E. Fujii (The University of Tokyo, Japan) for preparing FIB samples for TEM observation, and Mr. S. Nakamura (Material Analysis Suzukake-dai Center, Tokyo Institute of Technology, Japan) for ICP-AES measurements.

References

- 1 N. W. Emanetoglu, C. Gorla, Y. Liu, S. Liang, Y. Lu, *Mater. Sci. Semicond. Process.*, 1999, **2**, 247-252.
- 2 M. H. Huang, S. Mao, H. Feick, H. Yan, Y. Wu, H. Kind, E. Weber, R. Russo, P. Yang, *Science*, 2001, **292**, 1897-1899.
- 3 N. Saito, H. Haneda, T. Sekiguchi, N. Ohashi, I. Sakaguchi, K. Koumoto, *Adv. Mater.*, 2002, **14**, 418- 421.
- 4 S. Liang, H. Sheng, Y. Liu, Z. Huo, Y. Lu, H. Shen, *J. Cryst. Growth*, 2001, **225**, 110-113.
- 5 Y. Lin, Z. Zhang, Z. Tang, F. Yuan, J. Li, *Adv. Mater. Opt. Electron.*, 1999, **9**, 205-209.
- 6 N. Golego, S. A. Studenikin, M. Cocivera, *J. Electrochem. Soc.*, 2000, **147**, 1592-1594.
- 7 K. Keis, E. Magnusson, H. Lindstrom, S. E. Lindquist, A. Hagfeldt, *Sol. Energy Mater. Sol. Cells*, 2002, **73**, 51-58.
- 8 N. Ohashi, K. Takahashi, S. Hishita, I. Sakaguchi, H. Funakubo, H. Haneda, *J. Electrochem. Soc.*, 2007, **154**, D82-D87.
- 9 A. McLaren, T. Valdes-Solis, G. Li, S. C. Tsang, *J. Am. Chem. Soc.*, 2009, **131**, 12540-12541.
- 10 E. S. Jang, J.-H. Won, S.-J. Hwang, J.-H. Choy, *Adv. Mater.*, 2006, **18**, 3309–3312.
- 11 K. Matsumoto, N. Saito, T. Mitate, J. Hojo, M. Inada, H. Haneda, *Cryst. Growth Des.*, 2009,

- 9, 5014-5016.
- 12 X. Wang, P. Hu, F. L. Yuan, L. J. Yu, *J. Phys. Chem. C*, 2007, **111**, 6706-6712.
- 13 J. X. Duan, X. T. Huang, E. K. Wang, H. H. Ai, *Nanotechnology*, 2006, **17**, 1786-1790.
- 14 X.W. Lou, L.A. Archer, Z. Yang, *Adv. Mater.*, 2008, **20**, 3987-4019.
- 15 K. An, T. Hyeon, *NanoToday*, 2009, **4**, 359-373.
- 16 J. Zhang, S. Wang, Y. Wang, M. Xu, H. Xia, S. Zhang, W. Huang, X. Guo, S. Wu, *Sens. Actuators B: Chem.*, 2009, **139**, 411-417.
- 17 H. Zhou, T. X. Fan, D. Zhang, *Microporous Mesoporous Mater.*, 2007, **100**, 322-327.
- 18 H. Qian, G. Lin, Y. Zhang, P. Guanwan, R. Xu, *Nanotechnology*, 2007, **18**, 355602.
- 19 P. X. Gao, Z. L. Wang, *J. Am. Chem. Soc.*, 2003, **125**, 11299-11305.
- 20 G. Shen, Y. Bando, C.-J. Lee, *J. Phys. Chem. B*, 2005, **109**, 10578-10583.
- 21 H. Lu, L. Liao, J. Li, D. Wang, H. He, Q. Fu, L. Xu, Y. Tian, *J. Phys. Chem. B*, 2006, **110**, 23211-23214.
- 22 Y. Yang, Y. Chu, Y. Zhang, F. Yang, J. Liu, *J. Solid State Chem.*, 2006, **179**, 470-475.
- 23 S. Cheng, D. Yan, J. T. Chen, R. F. Zhuo, J. J. Feng, H. J. Li, H. T. Feng, P. X. Yan, *J. Phys. Chem. C*, 2009, **113**, 13630-13635.
- 24 Y. F. Zhu, D. H. Fan, W. Z. Shen, *J. Phys. Chem. C*, 2007, **111**, 18629-18635.
- 25 Q. Li, E. Wang, S. Li, C. Wang, C. Tian, G. Sun, J. Gu, R. Xua, *J. Solid State Chem.*, 2009,

- 182**, 1149-1155.
- 26 P. Hu, X. Zhang, N. Han, W. Xiang, Y. Cao, F. Yuan, *Cryst. Growth Des.*, 2011, **11**, 1520-1526.
- 27 Y. Qiu, W. Chen, S. Yang, B. Zhang, X. X. Zhang, Y. C. Zhong, K. S. Wong, *Cryst. Growth Des.*, 2010, **10**, 177-183.
- 28 K. Govender, D. S. Boyle, P. B. Kenway, P. O'Brien, *J. Mater. Chem.*, 2004, **14**, 2575-2591.
- 29 X. W. Lou, Y. Wang, C. Yuan, J. Y. Lee, L. A. Archer, *Adv. Mater.*, 2006, **18**, 2325-2329.
- 30 T. Ghoshal, S. Kar, S. Chaudhuri, *Cryst. Growth Des.*, 2007, **7**, 136-141.
- 31 S. Cheng, D. Yan, J. T. Chen, R. F. Zhuo, J. J. Feng, H. J. Li, H. T. Feng, P. X. Yan, *J. Phys. Chem. C*, 2009, **113**, 13630-13635.
- 32 M. K. Lee, H. F. Tu, *J. Appl. Phys.*, 2007, **101**, 126103.
- 33 H. Zeng, G. Duan, Y. Li, S. Yang, X. Xu, W. Cai, *Adv. Funct. Mater.*, 2010, **20**, 561-572.
- 34 H.-M. Cheng, H.-C. Hsu, Y.-K. Tseng, L.-J. Lin, W.-F. Hsieh, *J. Phys. Chem. B*, 2005, **109**, 8749-8754.
- 35 N. Y. Garces, L. Wang, L. Bai, N. C. Giles, L. E. Halliburton, *Appl. Phys. Lett.*, 2002, **81**, 622-624.
- 36 A. B. Djurisic, Y. H. Leung, K. H. Tam, Y. F. Hsu, L. Ding, W. K. Ge, Y. C. Zhong, K. S.

Wong, W. K. Chan, H. L. Tam, K. W. Cheah, W. M. Kwok, D. L. Phillips, *Nanotechnology*,

2007, **18**, 095702.

Figure Captions

Figure 1. SEM images of ZnO particles prepared at 150 °C for (a) 1, (c) 3, (e) 6 and (g) 12 h, and their higher magnification views in (b), (d), (f) and (h), respectively.

Figure 2. Particle size distributions of spheres prepared at 150 °C for different reaction times.

Figure 3. TEM images of top views of ZnO microspheres prepared at 150 °C for (a) 3, (b) 6 and (c) 12 h.

Figure 4. SEM images of ZnO prepared from reaction times of (a) 3 and (d) 12 h at 150°C, and their corresponding cross-sectional TEM images in (b) and (e), respectively. (c) HR-TEM image of the circled area in (b).

Figure 5. ICP-AES analysis of the variation in supernatant Zn concentration after various reaction times.

Figure 6. SEM images of ZnO microspheres prepared at (a) 100 and (c) 200 °C for 12 h, and their corresponding high magnification images in (b) and (d), respectively.

Figure 7. SEM images of ZnO microspheres prepared at 200 °C for (a) 1 and (d) 4 h, and their corresponding cross-sectional TEM images in (b) and (e), respectively. (c) and (f) HR-TEM images of the particle surfaces shown inset in (b) and (e), respectively.

Figure 8. Proposed formation mechanism of the ZnO hollow spheres.

Figure 9. PL spectrum of ZnO hollow microspheres prepared at 150 °C for 12 h.

Figure 1.

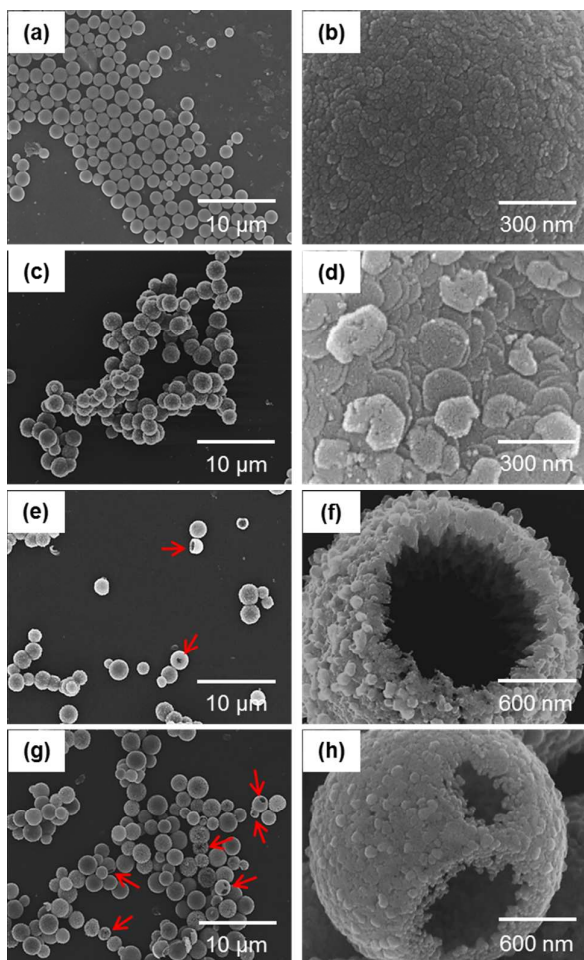


Figure 2.

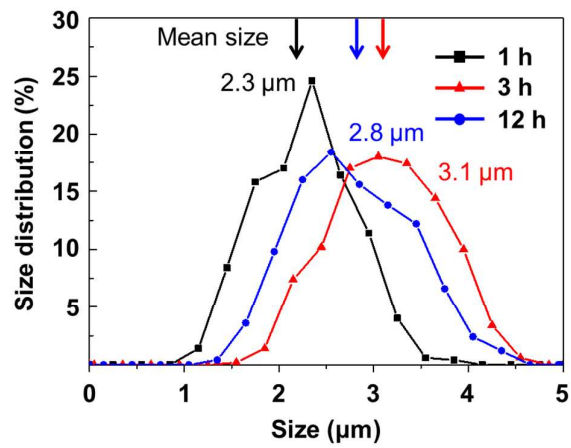


Figure 3.

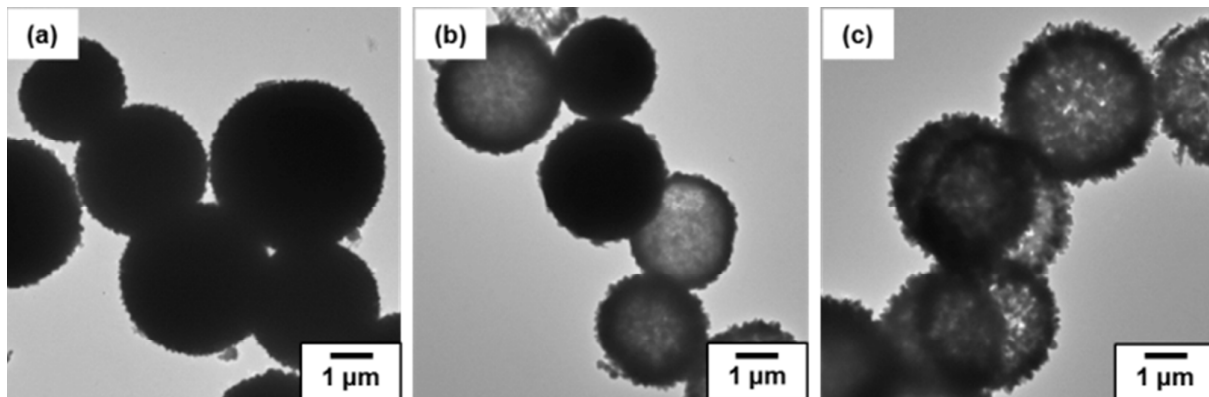


Figure 4.

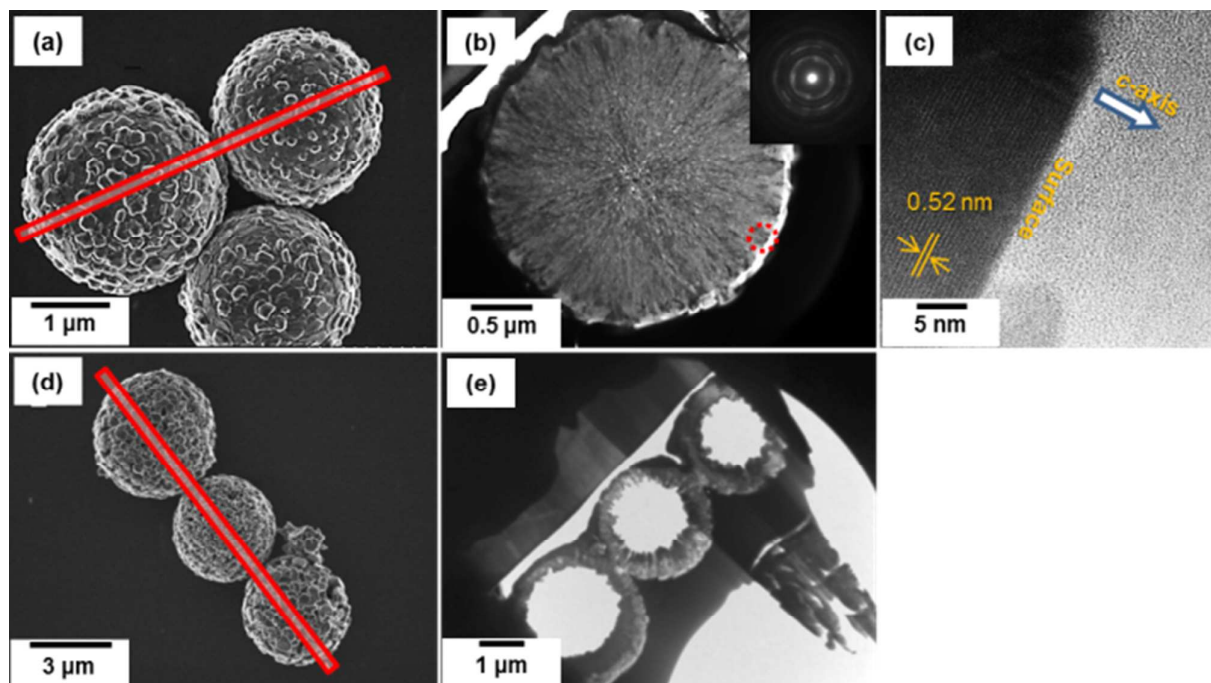


Figure 5.

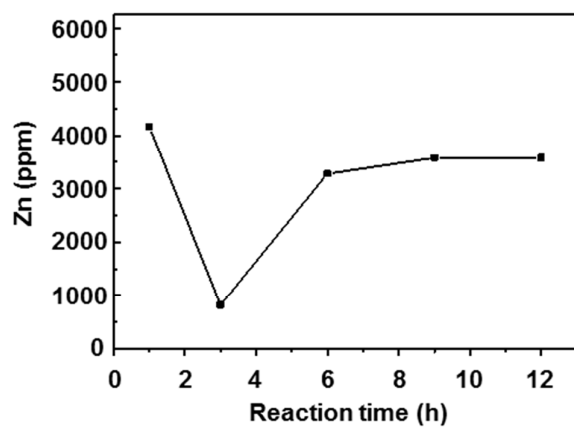


Figure 6.

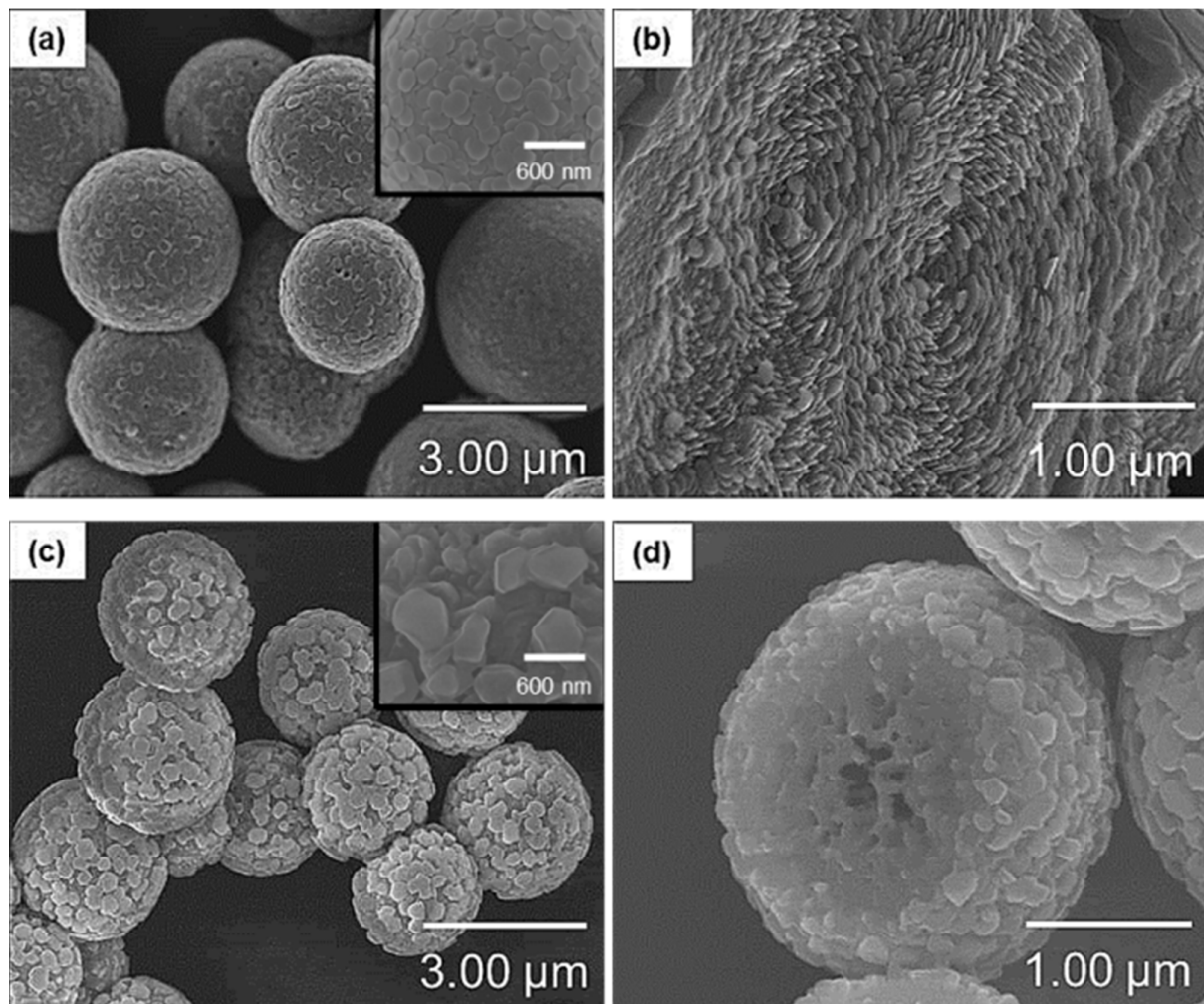


Figure 7.

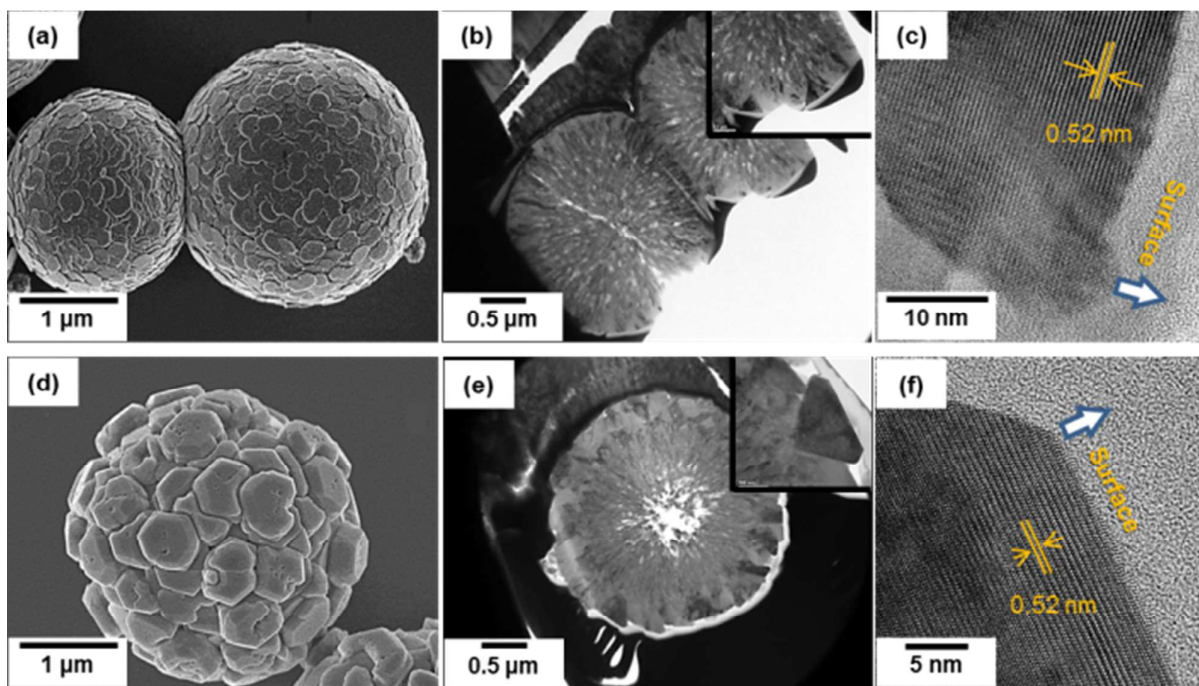


Figure 8.

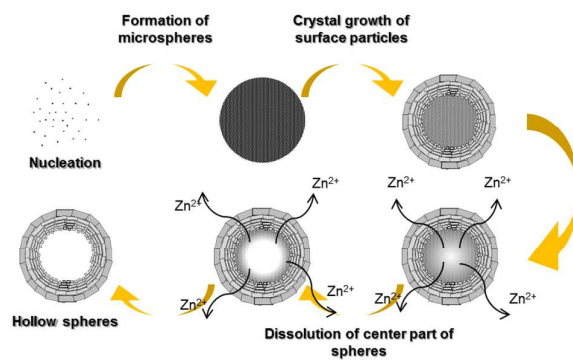


Figure 9.

